



Published in final edited form as:

*Chem Commun (Camb)*. 2014 December 11; 50(95): 15105–15108. doi:10.1039/c4cc07004f.

## Self-Folded Redox/Acid Dual-Responsive Nanocarriers for Anticancer Drug Delivery

Yue Lu<sup>a,b</sup>, Ran Mo<sup>a,b</sup>, Wanyi Tai<sup>a,b</sup>, Wujin Sun<sup>a,b</sup>, Dennis B. Pacardo<sup>a,b</sup>, Chenggen Qian<sup>a,b,c</sup>, Qundong Shen<sup>c</sup>, Frances S. Ligler<sup>a</sup>, and Zhen Gu<sup>a,b,\*</sup>

<sup>a</sup> Joint Department of Biomedical Engineering, University of North Carolina at Chapel Hill and North Carolina State University, Raleigh, NC, 27695, USA.

<sup>b</sup> Center for Nanotechnology in Drug Delivery and Division of Molecular Pharmaceutics, UNC Eshelman School of Pharmacy, University of North Carolina at Chapel Hill, Chapel Hill, NC, 27599, USA.

<sup>c</sup> Department of Polymer Science & Engineering, School of Chemistry & Chemical Engineering, Nanjing University, Nanjing, China.

### Abstract

Self-folded redox/acid dual-responsive nanocarriers (RAD-NCs) are developed for physiologically triggered delivery of anticancer drug. The evidenced redox/acid responsiveness, facile decoration of ligands, and active tumor-targeting capability of RAD-NCs suggest their potential as a promising formulation for tumor-targeted chemotherapy.

The last decades have witnessed vast efforts being put into the design of versatile anticancer drug delivery systems for precise “on demand” release and enhanced therapeutic efficacy.<sup>1-2</sup> The distribution of conventional chemotherapeutic agents is nonspecific in the body where they affect both cancerous and normal cells, thereby limiting the achievable dose within the tumor and also leading to suboptimal treatment due to excessive toxicities.<sup>3</sup> In light of this, delivery approaches based on smart stimuli-responsive materials have drawn extensive attention these years.<sup>1, 4-7</sup> Various nanomaterials and formulations have been engineered and tailored with integration of stimuli triggers.<sup>8-15</sup> Recently, there has been a growing interest in designing and developing smart drug delivery systems with the ability to respond to dual or multiple stimuli, thereby assuring drug release under complex pathological conditions with fine-tuned drug release profile to augment therapeutic efficacy.<sup>16-18</sup> Numerous nanomaterials with dual or multi-sensitivities, such as pH/temperature, pH/redox, pH/glucose, pH/enzyme, dual enzyme, enzyme/light have been developed and studied.<sup>19-25</sup> For example, the endosomal acidification can be utilized as a trigger for endosomal escape and the release of encapsulated drugs.<sup>26-28</sup> While glutathione (GSH), a tripeptide, is found at 2 to 3 orders higher level (approximately 2-10 mM) in the cytosol than in the extracellular fluids (approximately 2-20  $\mu$ M), rendering the relatively low intracellular redox

potential.<sup>29-32</sup> Therefore a combination design integrating pH and redox responsive elements can significantly enhance therapeutic efficacy.<sup>33-35</sup>

In this communication, we developed a novel redox/acid dual-responsive nanocarrier (RAD-NCs) with a well-defined core-shell structure capable of targeted delivery of the broad-spectrum anticancer drug doxorubicin (DOX) to cancer cells. As shown in **Figure 1**, the RAD-NCs were assembled from a graft copolymer mainly comprised of polyethylene glycol (PEG) and polyserine, which are highly biocompatible. As a commonly used non-ionic hydrophilic polymer, PEG possesses a lot of advantages favoring its application in the design and development of polymer-based drug delivery systems.<sup>36</sup> Different from traditional redox responsive formulations using redox-responsive disulfide-containing cross-linkers, the disulfide bonds were directly incorporated into the PEG backbone as a shell component; while highly acidic-sensitive hydrophobic ketal groups were introduced to the polyserine side chain (designated *m*-polyserine). DOX was non-covalently encapsulated in the hydrophobic core during a self-folding process due to the amphiphilic nature of the copolymer. Additionally, the pendant acid-labile ketals on the polyserine segment sheds upon acidic hydrolysis, which renders the resulting PEG-polyserine water soluble,<sup>37</sup> leading to the pH-responsive release of the encapsulated DOX.

Attributed to the reversible characteristic of thiol-disulfide chemistry, disulfide bonds are often incorporated into the design and development of redox-responsive nanomaterials.<sup>38</sup> Herein, the disulfide bond was directly incorporated into the polymeric backbone *via* a condensation polymerization in our design.<sup>39-40</sup> Importantly, these disulfide bonds not only served as a redox-sensitive moiety, but also provided potential for further modification of the RAD-NCs surface such as conjugation of tumor-targeting ligand, as they can be facilely utilized as reaction site. Folic-acid moiety, the receptor of which is overexpressed on the surface of various types of tumor cells, is decorated into the polymeric shell for enhanced cellular uptake and nuclear localization of the DOX loaded RAD-NCs. The insertion of folic-acid moiety is achieved using a facile two-step procedure (**Figure 1-A**). Antioxidant GSH (0.5 mM) was first added into the RAD-NCs solution to partially break the disulfide linkers, followed by purification and addition of folic acid-polyethylene glycol-maleimide (folic acid-PEG-maleimide) for conjugation with the thiol group. The DOX loaded FA-RAD-NCs are expected to enhance anticancer efficacies of DOX due to its two-phase release kinetics and synergetic effect of folic-acid targeting.

The graft copolymer for assembling RAD-NCs was synthesized *via* a two-step polymerization as illustrated in **Figure S1**. Monomer I, *N,N*-bis(2-aminoethyl)-*N*-[2-(tert-butylcarbonyl)ethyl]-amine, was synthesized as reported.<sup>41-42</sup> As a connection, partially protected tris(2-aminoethyl)amine (monomer I) condensed with bifunctional NHS-PEG5000-NHS (monomer II) and NHS-PEG-SS-PEG-NHS (monomer III) to form a multiblock copolymer. After removing the protective Boc group, the third amino group on the connection was liberated and served as the initiator for side-chain polymerization.<sup>43</sup> The molecular weight of the resulting linear backbone was assayed using the gel permeation chromatography (GPC), and this linear block copolymer displays a narrow distributed molecular weight at 78,064 g/mol. The ring-opening polymerization (ROP) of amino acid *N*-carboxyanhydrides (monomer IV, **Figure S2**), facilitated by *N*-Trimethylsilyl (TMS),

gradually proceeded on the main chain, leading to the structurally well-defined graft copolymer, which is sensitive to both pH and redox potential.<sup>44-45</sup>

To fold the graft copolymer and encapsulate DOX, DOXHCl was dissolved into dimethyl sulfoxide (DMSO) together with TEA under stirring, followed by the addition of homogenous graft copolymer solution. The mixture was then simply mixed with large quantities of water under vigorously stirring. Together with DOX encapsulation, the folding was processed instantly and efficiently. Within the folding process of graft copolymer, as much as 23.1 wt% of DOX (percentage of DOX weight compared to the total weight) can be encapsulated into the nanocarriers. The transmission electron microscopy (TEM) image of RAD-NCs appeared as monodispersed particles with a diameter of around 200 nm, which was in good agreement with the results determined by the dynamic laser scattering (DLS) assay (**Figure 2**), while no significant size and morphology changes were observed with DOX encapsulation (**Figure S3**). The zeta potential of RAD-NCs and DOX/RAD-NCs were -0.651 mV and -0.372 mV, respectively. The loading capacity of DOX under this condition was ~ 16.7 wt% of the total weight.

To evaluate the redox/acid sensitivities of RAD-NCs, reducing and acidic conditions mimicking the intracellular environment were performed. To study the dual-responsive conformational changes of RAD-NCs, nanocarriers were treated with GSH (10 mM), acid (pH 5.0) and GSH/acid, respectively. The corresponding conformational changes after 24 h were further monitored using the TEM imaging. According to **Figure 3-A**, the treatment of GSH (10 mM), acid (pH 5.0) and the combination of GSH and acid all led to the degradation of RAD-NCs, confirming the redox/acid sensitivities of RAD-NCs. These results suggested that RAD-NCs were capable of undergoing degradation in response to the intracellular microenvironment, indicating their potential for stimuli-triggered intracellular drug release.

The drug release profile of RAD-NCs upon acid and redox gradient was assessed in phosphate-buffered saline (PBS, 0.1 M) and acetate buffer with and without GSH (1 mM and 10 mM) at 37 °C, respectively. The relevant results were summarized in **Figure 3B**. As expected, the release rate of DOX in PBS (pH 7.4) was much slower than that in acetate buffer (pH 5.0). About 14.0% and 24.0% of DOX was released from the nanocarriers in the first 5 h at pH 7.4 and 5.0, respectively. DOX could be further released from RAD-NCs at pH 5.0 and achieved 71.7% after 48 h, while the released DOX was only 38.9% for nanocarriers incubated at pH 7.4 over the same time period. The amount of DOX released from the nanoparticles was promptly increased when it was incubated in the medium supplemented with 10 mM GSH, but the release profiles were similar to those in the plain media. At 48 h, the amount of DOX released from the nanoparticles was 84.2% and 94.0% at pH 7.4 and 5.0 in the presence of 10 mM GSH, respectively. It should be noted that even the low GSH concentration (1 mM) could notably enhance the release of DOX at both pH, indicating the superior redox-sensitivity of RAD-NCs, which could be attributed to the direct incorporation of disulfide bonds to the polymeric backbone of the nanocarriers, the cleavage of which highly promoted drug release. This finding was also consistent with the TEM results in **Figure 3-A**, which displayed that the incorporation of redox-triggered degradation significantly affected the integrity of nanocarriers. Furthermore, it was

suggested that the release of DOX from RAD-NCs displayed a two-phase pattern where an initial fast release phase was followed by a slow release phase.

Targeting moiety, folic acid was modified onto the surface of nanocarriers using a facile two-step procedure (**Figure 1-A**). GSH (0.5 mM) was first added into the RAD-NCs solution under stirring, followed by the addition of folic acid-PEG-maleimide. The RAD-NCs conjugated with folic acid moiety was observed using TEM (**Figure S4-A**). After targeting ligand conjugation, the nanocarriers maintained their redox and acid sensitivities (**Figure S4-C**). This is the first time that disulfide bonds have been incorporated onto the backbone of the polymeric nanocarrier for both the redox-sensitivity and the subsequent insertion of ligand for active targeting at tumor site.

The endocytosis pathway of DOX loaded RAD-NCs (DOX/RAD-NCs) was determined *via* pre-incubating human cervical carcinoma epithelial (HeLa) cells with several specific inhibitors of various kinds of endocytosis. As shown in **Figure S5**, sucrose (SUC, inhibitor of clathrin-mediated endocytosis), amiloride (AMI, inhibitor of macropinocytosis) and methyl- $\beta$ -cyclodextrin (MCD, inhibitor of lipid raft) all reduced the uptake of DOX/RAD-NCs significantly, which indicated DOX/RAD-NCs were taken up by HeLa cells *via* clathrin-mediated endocytosis, macropinocytosis and lipid raft, especially macropinocytosis.<sup>46-50</sup> In contrast, insignificant inhibition on the cellular uptake of nanocarrier was found in the cells pretreated with chlorpromazine (CPZ, inhibitor of clathrin-mediated endocytosis) and nystatin (NYS, inhibitor of caveolin-mediated endocytosis). Similar phenomenon was also observed in the cellular uptake of polymeric micelles.<sup>51</sup> These results indicated that clathrin-mediated endocytosis, macropinocytosis and lipid raft might play a major role in the internalization of the nanocarrier. The intracellular delivery of DOX/RAD-NCs and DOX/FA-RAD-NCs in HeLa cells was also explored using confocal laser scanning microscopy (CLSM). The fluorescence of DOX was clearly observed in HeLa cells after 1 h of incubation with DOX/RAD-NCs, which provided a visual evidence of the cellular internalization of DOX/RAD-NCs and the release of the loaded DOX molecules. When the incubation time was prolonged to 4 h, DOX was delivered and released into the nuclei of HeLa cells, as indicated by the magenta fluorescence (**Figure 4-A**). Similar pattern was observed in HeLa cells incubated with DOX/FA-RAD-NCs (**Figure 4-B, Figure S6**). The fluorescence intensity of DOX is significantly higher compared with DOX/RAD-NCs, which can be attributed to the active targeting ability of folic acid moiety.

To assess anticancer efficacy of RAD-NCs, DOX encapsulated nanocarriers was treated with HeLa cells and evaluated by 3-(4,5-dimethylthiazol-2-yl)-2,5-diphenyltetrazolium bromide (MTT) assay. As shown in **Figure 4-C, D**, cell viability was dependent on both DOX concentration and incubation time, as expected. The halfmaximal inhibitory concentration ( $IC_{50}$ ) of DOX/RAD-NCs and DOX/FA-RAD-NCs towards HeLa cells for 24 h treatment were  $2.5 \text{ mgL}^{-1}$  and  $0.9 \text{ mgL}^{-1}$ , respectively. Both DOX/RAD-NCs and DOX/FA-RAD-NCs have displayed higher cytotoxicity than free DOX solution (for 24 h treatment:  $IC_{50} = 2.6 \text{ mgL}^{-1}$ ). Interestingly, for 24 h treatment, DOX/FA-RADs didn't show enhanced cytotoxicity compared with free DOX solution. This might be attributed to the difference in surface property of the NCs caused by the introduction of folic acid targeting

moiety.<sup>52</sup> Empty RAD-NCs and FA-RAD-NCs without DOX did not show significant cytotoxicity within the tested range of concentrations (**Figure S7**). It was suggested that the controlled release of DOX achieved by redox/acid responsive RAD-NCs provided higher cytotoxic activity towards cancer cells. DOX/FA-RAD-NCs showed significantly enhanced cytotoxicity (2.8-fold for 24 h treatment) compared with DOX/RAD-NCs towards folic acid positive HeLa cells where folate receptor proteins were overexpressed, which can be attributed to the existence of folic acid targeting moiety.

In summary, we have developed a novel redox/acid dual responsive nano-vehicle for programmed anticancer drug delivery. Due to the synergetic effect of folic-acid targeting effect and its two-phase release kinetics, the anticancer efficacy of DOX/FA-RAD-NCs is significantly enhanced. The facile synthetic route, ease of decoration, high loading capacity of drug and synergistic degradation mechanism render this dual-responsive drug carrier a promising formulation for tumor-targeted chemotherapy.

## Supplementary Material

Refer to Web version on PubMed Central for supplementary material.

## Acknowledgements

This work was supported by the grant 550KR51307 from NC TraCS, NIH's Clinical and Translational Science Awards (CTSA) at UNC-CH and the NC State Faculty Research and Professional Development Award to Z.G.

## References

1. Mura S, Nicolas J, Couvreur P. *Nat. Mater.* 2013; 12:991. [PubMed: 24150417]
2. Davis ME, Chen Z, Shin DM. *Nat. Rev. Drug Discov.* 2008; 7:771. [PubMed: 18758474]
3. Ross JS, Schenkein DP, Pietrusko R, Rolfe M, Linette GP, Stec J, Stagliano NE, Ginsburg GS, Symmans WF, Pusztai L, Hortobagyi GN. *American journal of clinical pathology.* 2004; 122:598. [PubMed: 15487459]
4. Kim CS, Duncan B, Creran B, Rotello VM. *Nano today.* 2013; 8:439. [PubMed: 24159362]
5. Rapoport N. *Prog. Polym. Sci.* 2007; 32:962.
6. Gu Z, Yan M, Hu B, Joo K-I, Biswas A, Huang Y, Lu Y, Wang P, Tang Y. *Nano Lett.* 2009; 9:4533. [PubMed: 19995089]
7. Zhang Q, Re Ko N, Kwon Oh J. *Chem. Commun.* 2012; 48:7542.
8. Peer D, Karp JM, Hong S, Farokhzad OC, Margalit R, Langer R. *Nat. Nano.* 2007; 2:751.
9. Gu Z, Biswas A, Zhao M, Tang Y. *Chem. Soc. Rev.* 2011; 40:3638. [PubMed: 21566806]
10. Stuart MAC, Huck WTS, Genzer J, Muller M, Ober C, Stamm M, Sukhorukov GB, Szleifer I, Tsukruk VV, Urban M, Winnik F, Zauscher S, Luzinov I, Minko S. *Nat. Mater.* 2010; 9:101. [PubMed: 20094081]
11. Shim MS, Kwon YJ. *Adv. Drug Deliver. Rev.* 2012; 64:1046.
12. Li Y, Gao GH, Lee DS. *Adv. Healthcare Mater.* 2013; 2:388.
13. Mo R, Jiang T, Di J, Tai W, Gu Z. *Chemical Society Reviews.* 2014; 43:3595. [PubMed: 24626293]
14. Mo R, Jiang T, DiSanto R, Tai W, Gu Z. *Nat. Commun.* 2014; 5
15. Ding J, Chen L, Xiao C, Chen L, Zhuang X, Chen X. *Chem. Commun.* 2014
16. Slowing II, Vivero-Escoto JL, Wu CW, Lin VS. *Adv Drug Deliv Rev.* 2008; 60:1278. [PubMed: 18514969]

17. Cheng R, Meng F, Deng C, Klok HA, Zhong Z. *Biomaterials*. 2013; 34:3647. [PubMed: 23415642]
18. Jiang T, Mo R, Bellotti A, Zhou J, Gu Z. *Adv. Funct. Mater.* 2014; 24:2295.
19. Cheng R, Meng F, Deng C, Klok H-A, Zhong Z. *Biomaterials*. 2013; 34:3647. [PubMed: 23415642]
20. Gu Z, Biswas A, Joo K-I, Hu B, Wang P, Tang Y. *Chem. Commun.* 2010; 46:6467.
21. Chen X, Chen L, Yao X, Zhang Z, He C, Zhang J, Chen X. *Chem. Commun.* 2014; 50:3789.
22. Radhakrishnan K, Tripathy J, Raichur AM. *Chem. Commun.* 2013; 49:5390.
23. Lu Y, Sun W, Gu Z. *J. Control. Release*. 2014; 194:1. [PubMed: 25151983]
24. Hu Q, Katti PS, Gu Z. *Nanoscale*. 2014 doi: 10.1039/c4nr04249b.
25. Sun W, Jiang T, Lu Y, Reiff M, Mo R, Gu Z. *J. Am. Chem. Soc.* 2014 doi: 10.1021/ja5088024.
26. Liu T, Hu J, Jin Z, Jin F, Liu S. *Adv. Healthcare Mater.* 2013; 2:1576.
27. Wen S, Liu H, Cai H, Shen M, Shi X. *Adv. Healthcare Mater.* 2013; 2:1267.
28. Du J, Tang Y, Lewis AL, Armes SP. *J. Am. Chem. Soc.* 2005; 127:17982. [PubMed: 16366531]
29. Schafer FQ, Buettner GR. *Free Radic. Biol. Med.* 2001; 30:1191. [PubMed: 11368918]
30. Yu S, Ding J, He C, Cao Y, Xu W, Chen X. *Adv Healthc Mater.* 2014; 3:752. [PubMed: 24574261]
31. Zhao M, Biswas A, Hu B, Joo K-I, Wang P, Gu Z, Tang Y. *Biomaterials*. 2011; 32:5223. [PubMed: 21514660]
32. Zhao M, Hu B, Gu Z, Joo K-I, Wang P, Tang Y. *Nano today*. 2013; 8:11.
33. Dai J, Lin S, Cheng D, Zou S, Shuai X. *Angew. Chem. Int. Edit.* 2011; 50:9404.
34. Zhang J, Wu L, Meng F, Wang Z, Deng C, Liu H, Zhong Z. *Langmuir*. 2011; 28:2056. [PubMed: 22188099]
35. Chen J, Qiu X, Ouyang J, Kong J, Zhong W, Xing MMQ. *Biomacromolecules*. 2011; 12:3601. [PubMed: 21853982]
36. Knop K, Hoogenboom R, Fischer D, Schubert US. *Angew. Chem. Int. Edit.* 2010; 49:6288.
37. Gu Z, Aimetti AA, Wang Q, Dang TT, Zhang Y, Veiseh O, Cheng H, Langer RS, Anderson DG. *ACS Nano*. 2013; 7:4194. [PubMed: 23638642]
38. Meng F, Hennink WE, Zhong Z. *Biomaterials*. 2009; 30:2180. [PubMed: 19200596]
39. Cerritelli S, Velluto D, Hubbell JA. *Biomacromolecules*. 2007; 8:1966. [PubMed: 17497921]
40. Xu Y, Meng F, Cheng R, Zhong Z. *Macromol. Biosci.* 2009; 9:1254. [PubMed: 19904724]
41. van der Velden J, Narolska NA, Lamberts RR, Boontje NM, Borbely A, Zaremba R, Bronzwaer JG, Papp Z, Jaquet K, Paulus WJ, Stienen GJ. *Cardiovasc. Res.* 2006; 69:876. [PubMed: 16376870]
42. Benito JM, Gomez-Garcia M, Ortiz Mellet C, Baussanne I, Defaye J, Garcia Fernandez JM. *J Am Chem Soc.* 2004; 126:10355. [PubMed: 15315450]
43. Tai W, Chen Z, Barve A, Peng Z, Cheng K. *Pharm. Res.* 2014; 31:706. [PubMed: 24072263]
44. Lu H, Cheng J. *J. Am. Chem. Soc.* 2008; 130:12562. [PubMed: 18763770]
45. Lu H, Wang J, Lin Y, Cheng J. *J. Am. Chem. Soc.* 2009; 131:13582. [PubMed: 19725499]
46. Mo R, Sun Q, Xue J, Li N, Li W, Zhang C, Ping Q. *Adv. Mater.* 2012; 24:3659. [PubMed: 22678851]
47. Zhang XX, Allen PG, Grinstaff M. *Mol. Pharm.* 2011; 8:758. [PubMed: 21449536]
48. Rehman, Z. u.; Hoekstra, D.; Zuhorn, IS. *J. Control. Release*. 2011; 156:76. [PubMed: 21787817]
49. Koivusalo M, Welch C, Hayashi H, Scott CC, Kim M, Alexander T, Touret N, Hahn KM, Grinstein S. *J. Cell Biol.* 2010; 188:547. [PubMed: 20156964]
50. Chiu Y-L, Ho Y-C, Chen Y-M, Peng S-F, Ke C-J, Chen K-J, Mi F-L, Sung H-W. *J. Control. Release*. 2010; 146:152. [PubMed: 20580915]
51. Sahay G, Batrakova EV, Kabanov AV. *Bioconjugate Chem.* 2008; 19:2023.
52. Goren D, Horowitz AT, Tzemach D, Tarshish M, Zalipsky S, Gabizon A. *Clinical Cancer Research*. 2000; 6:1949. [PubMed: 10815920]



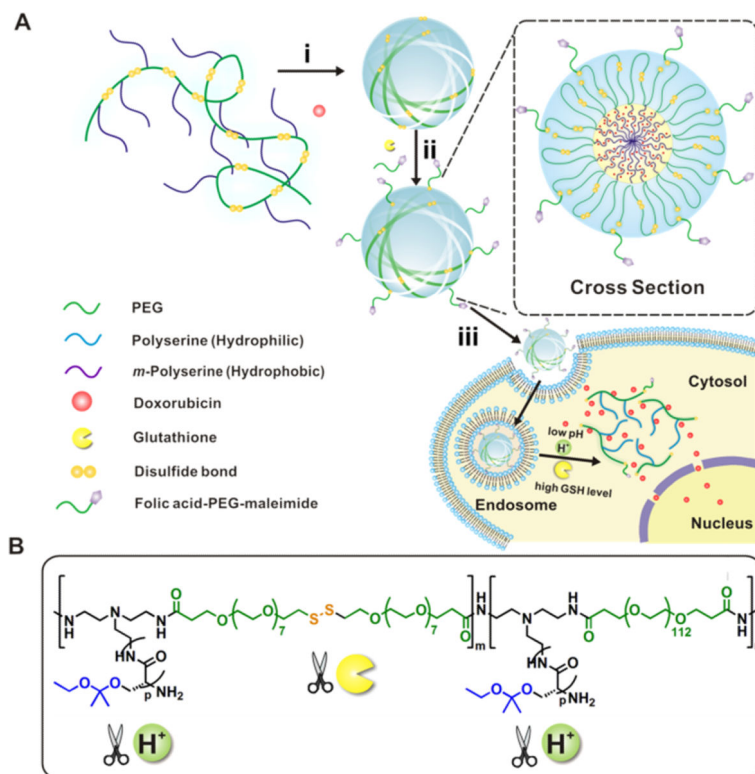


**Figure 1.** Schematic design of the redox/acid dual-responsive nanocarriers (RAD-NCs) for anticancer drug delivery. A) Schematic illustration of the formation and structural transitions of RAD-NCs for targeted intracellular drug delivery. i) Self-assemble the graft copolymer with DOX into nanocarriers; ii) decoration of the targeting ligand (folic acid) with thiol groups generated by partial cleavage of disulfide using glutathione; iii) intracellular delivery of RAD-NCs. B) Schematic of the chemical structure of the graft copolymer and DOX. The scissors represent cleavage sites.

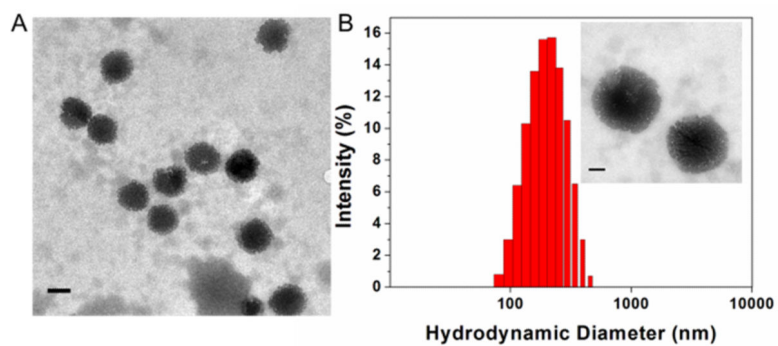


**Figure 2.** Characterization of graft; copolymer and nanocarriers. A) Representative TEM image of RAD-NCs. Scale bar: 200 nm. B) Hydrodynamic size of RAD-NCs measured by DLS. Inset: TEM image of RAD-NCs (zoom in). Scale bar: 100 nm.



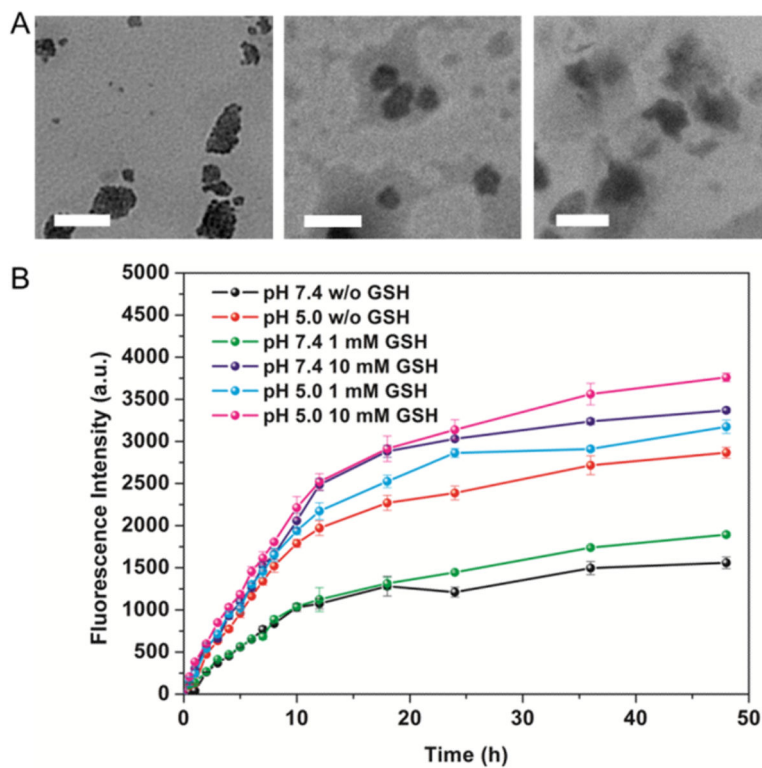


**Figure 3.** A) Representative TEM images of nanocarriers treated with GSH (10 mM) and acid (pH 5.0): GSH (left), acid (middle) and GSH/acid (right). Scale bars: 200 nm. B) DOX release profiles of DOX-loaded micelles in different buffers at 37 °C. Data represent mean  $\pm$  SD (n=3).

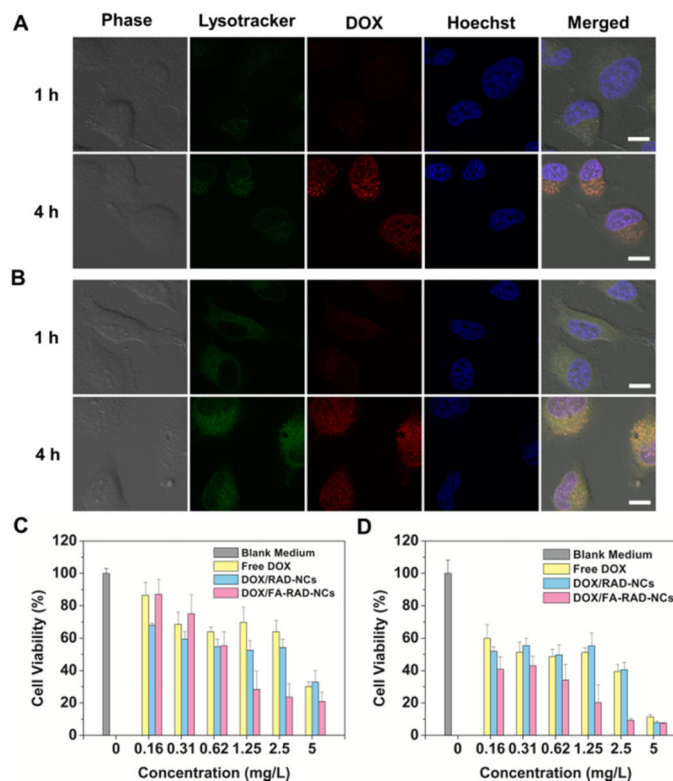


**Figure 4.**

The cellular uptake behavior and cytotoxicity of DOX/RAD-NCs and DOX/FA-RAD-NCs toward HeLa cell line. (A, B) Intracellular trafficking of DOX/RAD-NCs (A) and DOX/FA-RAD-NCs (b) on HeLa cell line observed by CLSM. The late endosomes and lysosomes were stained by LysoTracker Green, and the nuclei were stained by Hoechst 33342. Scale bar: 10  $\mu\text{m}$ . (C, D) Viabilities of HeLa cells incubated with blank medium, free DOX, DOX/RAD-NCs and DOX/FA-RAD-NCs at various DOX concentrations for C) 24 h and D) 48 h. The horizontal ordinate indicates the concentration of DOX. Error bars indicate s.d. ( $n=4$ ).